

Elsevier required licence: © <2019>. This manuscript version is made available under the CC-BY-NC-ND 4.0 license <http://creativecommons.org/licenses/by-nc-nd/4.0/>

The definitive publisher version is available online at

[\[https://www.sciencedirect.com/science/article/pii/S0301479719309429?via%3Dihub\]](https://www.sciencedirect.com/science/article/pii/S0301479719309429?via%3Dihub)

# Understanding the organic micro-pollutants transport mechanisms in the fertilizer-drawn forward osmosis process

Youngjin Kim <sup>a</sup>, Sheng Li <sup>a,b</sup>, Sherub Phuntsho <sup>c</sup>, Ming Xie <sup>d</sup>, TorOve Leiknes <sup>a</sup>, Johannes Vrouwenvelder <sup>a</sup>, Ho Kyong Shon <sup>c\*</sup>, Noreddine Ghaffour <sup>a\*</sup>

<sup>a</sup> King Abdullah University of Science and Technology (KAUST), Water Desalination and Reuse Center (WDRC), Division of Biological & Environmental Science & Engineering (BESE), Thuwal 23955-6900, Saudi Arabia

<sup>b</sup> Guangzhou Institute of Advanced Technology, Chinese Academy of Science, Haibin Road #1121, Nansha district, Guangzhou, China

<sup>c</sup> Centre for Technology in Water and Wastewater, School of Civil and Environmental Engineering, University of Technology Sydney (UTS), Post Box 129, Broadway, NSW 2007, Australia

<sup>d</sup> Institute for Sustainability and Innovation, College of Engineering and Science, Victoria University, PO Box 14428, Melbourne, Victoria, 8001, Australia

---

\* Co-corresponding authors.

Hokyong Shon. Tel.: +61-2-9514-2629; E-mail: Hokyong.Shon-1@uts.edu.au

Noreddine Ghaffour. E-mail: noreddine.ghaffour@kaust.edu.sa

## Highlights

- Performance of FDFO was significantly affected by the property of fertilizer DS.
- OMPs transport was governed by physicochemical property at low water flux and RSF.
- DAP reduced OMPs flux due to enhanced steric hindrance by increased FS pH and RSF.
- Transport of OMPs having high molecular weight was readily hampered by high RSF.
- The pore hindrance model could be helpful in understanding OMPs transport in FDFO.

## **Abstract**

This study systematically investigated the transport mechanism of organic micro-pollutants (OMPs) in a fertilizer-drawn forward osmosis (FDFO) membrane process. Four different OMPs were chosen as representatives due to their different molecular weights and structure characteristics. FDFO experiments were carried out under active layer facing feed solution using three different fertilizer draw solutions (DS): ammonium phosphate monobasic (MAP), ammonium phosphate dibasic (DAP) and potassium chloride (KCl). KCl showed the highest water flux and RSF while MAP and DAP exhibited similar water flux with varying RSF. The pH of the feed solution (FS) with DAP DS was increased due to the reverse diffusion of  $\text{NH}_4^+$  ions from the DS. The OMPs transport behavior was then evaluated in terms of OMPs flux and compared with simulated OMPs flux obtained via the pore hindrance transport model to identify the effect of OMPs structure on its transports. When using MAP DS, OMPs flux was dominantly influenced by their physicochemical properties (i.e., hydrophobicity and surface charge). With DAP DS, more hydrated FO membrane by increased pH as well as enhanced reverse salt flux (RSF) could strengthen the hinderance effect on the OMPs transport through FO membrane. With KCl DS, the sturcutre properties of OMPs were dominant factors for OMPs flux but remarkably increased RSF could hamper the transport of OMPs with high molecular weight. The pore hindrance model could be instrumental for understanding the effects of the hydrodynamic properties and the surface properties on the OMPs transport behaviors.

**Keywords:** Fertilizer-drawn forward osmosis; Organic micro-pollutants; Fertilizer properties; OMPs properties; The pore hindrance model

## 1. Introduction

In the last decades, organic micro-pollutants (OMPs), originating from pharmaceutical and personal care products (PPCPs), herbicides and pesticides, and industries, have been a problem because of their potential harmful impacts on public health and the environment via their bioaccumulation [1-3]. Despite the significance of OMPs on environments, there have been no legal discharge limits for OMPs in most countries but a few countries monitor and manage OMPs discharge through the watch list [4]. In addition, the direct reuse of wastewater, particularly in the agricultural sector, can be also restricted due to the presence of OMPs in raw sewage [5] even though wastewater reuse can be very important in sustaining freshwater resources and contribute to an appreciable amount of necessary nutrients for plants [6]. Therefore, OMPs in wastewater should be effectively removed for both reuse and discharge of wastewater.

Conventional biological treatment technologies such as, the activated sludge treatment have been applied for wastewater treatment. Their efficiencies on OMPs removal via biodegradation, sorption onto sludge flocs and volatilization are reported to range between 0% and 90% depending on OMPs properties, sludge properties and operating conditions, which potentially limits the reuse of wastewater [7-11]. To enhance the efficiency of the biological treatment, membrane bioreactor (MBR) has been proposed by combining a bioreactor with microfiltration (MF) or ultrafiltration (UF) because of low footprint, high effluent quality and complete rejection of suspended solids. MBR could be effective in the treatment of OMPs which were not readily removed by the activated sludge treatment process [7, 11, 12]. However, when considering the permissible limit, for instance 1 µg/L for irrigation reuse [13], these technologies may not produce adequate water reuse quality. Wastewater reuse is commonly considered to be more cost effective and environmentally friendly than seawater desalination or long-distance water transfers for regions experiencing regular

droughts and water scarcity [14]. For the wastewater reuse, therefore, advanced membrane processes (e.g., nanofiltration (NF) and reverse osmosis (RO)) have been often employed to enhance the removal efficiency since most OMPs, even at very low concentration levels, may have a negative effect on the environment [1, 15, 16]. Ionic OMPs could be easily rejected by the negatively charged membrane surface while the rejection of hydrophobic nonionic OMPs can continuously decrease with operation [17]. Besides, the rejection of positively charged OMPs was lower than that of negatively charged OMPs with similar molecular sizes [15]. Both NF and RO could achieve high rejections of OMPs but deteriorations in retentions on NF and RO membranes were reported for some OMPs, implying that its reuse can represent a possible risk implication [16]. Furthermore, the pressure-driven membrane processes, such as, NF or RO, can be highly disadvantaged by high energy consumption and severe membrane fouling due to the need to operate the process at high hydraulic pressure as a driving force [18]. To overcome these problems, forward osmosis (FO) has been proposed as an alternative to the conventional pressure based membrane desalting processes [19].

FO utilizes high concentration gradient as a driving force and in addition to generating higher water flux it also results in the reverse diffusion of draw solutes towards the feed water. As the reverse solute flux (RSF) of the draw solutes occurs in the direction opposite to that of the OMP solute flux, it provides a hinderence effect to the OMP flux and as a result, FO process has been reported to have a higher OMPs removal efficiency compared to RO process [20, 21]. Operation conditions (i.e., water flux, solution pH, membrane orientation and working temperature) also have a significant influence on the OMPs rejections in the FO process [22, 23]. The OMPs removal efficiencies by FO process under the active layer facing DS (AL-DS) mode of membrane orientation were much lower than those under the active layer facing FS (AL-FS) mode. This is

due to concentrative internal concentration polarization (ICP) in the support layer in which the back diffusion of the are severely restricted within the support layer thereby enhancing the OMPs flux and hence lowering the removal efficiency [23, 24]. The OMPs rejection decreases at higher FS temperature due to an increase in OMPs diffusivity, while the oppoiste effect is observed at higher DS temperature. The OMPs rejection increases at higher DS temperature as a result of the higher dilution effect enhanced by the increased water flux, the hindrance effect by the increased reverse salt flux [22]. The rejection of ionic OMPs is also significantly influenced by solution pH [25]. The thin-film composite (TFC) polyamide (PA) FO membrane is reported to have higher OMPs rejection due to pore hydration even though TFC membranes have bigger pore size compared to cellulose triacetate (CTA) based FO membranes [26]. OMPs rejection could be significantly influenced by membrane fouling and the initial water flux was oserved to be the key factor on both membrane fouling and OMPs rejection [23, 27]. Fouled FO membrane could also influence OMPs rejection depending on the surface characteristics of the fouling layer [28]. However, since FO process simply converts concentrated DS into a diluted DS, an additional desalting processes (e.g., NF, RO or membrane distillation) are required to extract pure water from the diluted DS [29].

Recently, fertilizer-drawn forward osmosis (FDFO) has received increased attention since the diluted fertilizer solution could be utilized directly for irrigation purpose without the need of a separation and recovery process [30, 31]. The FDFO has been employed by integrating with anaerobic MBR (AnMBR) for irrigation reuse [32] and it was effective in successfully concentrating the municipal wastewater [33]. However, high reverse diffusion of inorganic fertilizers towards the bioreactor is one of the major concnrs as it exhibited negative impact on the anerobic microorganisms, resulting a reduction of biogas production [34, 35]. Biofouling on the

osmotic membrane surface was considerably influenced by the properties of the fertilizers used as DS [36]. Nevertheless, FDFO has been found feasible for wastewater treatment and it has exhibited higher OMPs removal during treatment of AnMBR effluent [37]. Besides, when commercial hydroponic solution was evaluated as a DS, the diluted fertilizer solution produced by pilot FDFO has been found suitable for hydroponic application [38]. Despite the recent efforts to understand the FDFO process for wastewater treatment, the OMPs transport mechanisms in the FDFO process have not been well elucidated yet.

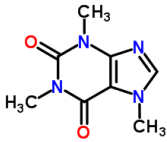

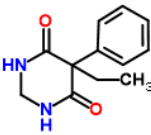
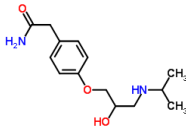
The aim of this study is therefore to investigate OMPs transport mechanisms in the FDFO process. Atenolol, atrazine, primidone, and caffeine were utilized as representatives of OMPs to investigate the effects of molecular weights and physicochemical properties (i.e., hydrophobicity and surface charge) of OMPs. Caffeine and primidone were compared due to their different molecular weights as well as similar surface physicochemical properties (i.e., neutral surface charges and similar hydrophobicity). Atrazine and primidone were also examined since they have different hydrophobicity while they have similar molecular weights and neutral surface charges. Atenolol was lastly selected to examine the effect of the surface charge (positive charge) on OMPs transport behaviors. To identify the effect of OMPs surface physicochemical properties on OMPs transports, the pore hindrance transport model was employed and compared to experimental data since this model has been utilized to estimate rejections by size exclusion [39]. This study has potential implications for the optimization of FDFO for the wastewater treatment.

## **2. Materials and methods**

## 2.1 Representative organic micro-pollutants (OMPs)

Four different OMPs (atenolol, atrazine, caffeine and primidone), received in powder form from Sigma Aldrich (Saudi Arabia), were used as representative OMPs. Their key properties are provided in **Table 1**. Diffusivity was calculated based on the Wilke and Chang equation and stokes radius was calculated using the Stokes-Einstein equation [40]. Stock solution with a final concentration of 4 g/L (i.e., 1 g/L for each OMP) was prepared by dissolving 4 mg of OMP compounds (i.e., 1 mg for each OMP) in 1 mL of pure methanol. The stock solution was then stored in a refrigerator at 4 °C prior to the experiments.

**Table 1.** Key physicochemical properties of OMPs used in this study.

	Caffeine	Atrazine	Primidone	Atenolol
Structure <sup>a</sup>				
Application	Stimulant	Herbicide	Anticonvulsant	Beta-blocker
Formula	C <sub>8</sub> H <sub>10</sub> N <sub>4</sub> O <sub>2</sub>	C <sub>8</sub> H <sub>14</sub> ClN <sub>5</sub>	C <sub>12</sub> H <sub>14</sub> N <sub>2</sub> O <sub>2</sub>	C <sub>14</sub> H <sub>22</sub> N <sub>2</sub> O <sub>3</sub>
Molecular weight (g/mol)	194	216	218	266
Charge <sup>a</sup> (at pH 6.5)	Neutral	Neutral	Neutral	Positive
Log <i>D</i> <sup>a, b</sup> (at pH 6.5)	-0.63	2.64	0.83	-2.09
<i>pK</i> <sub>a</sub> <sup>a</sup>	0.52	2.27	12.26	9.6
Diffusivity <sup>c</sup> (×10 <sup>-10</sup> m <sup>2</sup> /s)	6.46	6.10	6.07	5.46
Stokes radius <sup>d</sup> (nm)	0.33	0.35	0.35	0.39

<sup>a</sup> Data from ChemSpider website (<http://www.chemspider.com>).

<sup>b</sup> Higher Log *D* value indicates higher hydrophobicity.

<sup>c</sup> Diffusivity was calculated using the Wilke and Chang equation at 20 °C [40].

<sup>d</sup> Stokes radius was calculated using Stokes-Einstein equation [40].



## 2.2 FO membrane and draw solutions

Cellulose triacetate (CTA) FO membranes embedded in a woven polyester mesh, provided by Hydration Technology Innovations, HTI (Albany, OR, USA), was used in this study. Membrane transport parameters of FO membrane were adopted from our previous study [32] and are presented in **Table S1**, Supplementary Data. Average pore radius and structural factors of FO membrane (**Table S2**, Supplementary Data) were employed from the other study [26] and utilized to solve the pore hindrance transport model. Membrane surface characteristics (i.e., contact angle, zeta potential and roughness) of the active layer of FO membrane are shown in **Table 2**. Surface contact angle was analyzed by a Sigma 701microbalance (KSV Instrument Ltd., Finland) interfaced with a PC for automatic control and data acquisition, and zeta potential was analyzed by a streaming current electrokinetic analyzer (SurPass, Anton Paar GmbH, Austria). Surface roughness was characterized by AFM imaging (PUCOStation AFM, Surface Imaging Systems, Germany) which was conducted in contact mode with silicon probes (APPNANO, Applied Nano Structures Inc., USA).

**Table 2.** Surface characteristics of HTI CTA FO membrane. Zeta potential was measured at pH 6.5 under 0.01 M KCl as a background electrolyte solution. Contact angle and roughness were carried out at pH 6.5 and room temperature.

	Contact angle	Zeta potential	Roughness
CTA FO membrane	79.5°	-6.87 mV	13.33 nm

Three different chemical fertilizers of reagent grade were used in this study (Sigma Aldrich, Saudi Arabia) and they consisted of mono-ammonium phosphate (MAP), di-ammonium phosphate

(DAP) and potassium chloride (KCl). DS was prepared by dissolving fertilizers in deionized (DI) water. Detailed information of fertilizer chemicals is provided in **Table S3**, Supplementary Data. Osmotic pressure, diffusivity and viscosity of three fertilizers were obtained by OLI Stream Analyzer 3.2 (OLI System Inc., Morris Plains, NJ, USA).

### **2.3 FDFO experiments**

All FDFO experiments were carried out using a lab-scale FO system described in our previous studies [31, 37]. The FO cell had two symmetric channels (i.e., 100 mm long, 20 mm wide and 3 mm deep) on both sides of the membrane each fed with FS and DS respectively. Variable speed gear pumps (Cole-Parmer, USA) were used to provide crossflows under co-current directions at a crossflow rate of 8.5 cm/s. Solution temperature was 20 °C. Both solutions were recirculated in a closed-loop system resulting in a batch mode process operation. The DS tank was placed on a digital scale and the weight changes were recorded by a computer in real time every 3 mins interval to determine water flux.

FDFO experiments were carried out under AL-FS mode at 1 M or 2 M fertilizer DS concentrations. Detailed descriptions of FDFO experiments are available elsewhere [37]. Crossflow velocities of DS and FS were set at 8.5 cm/s and temperature at 20 °C. FDFO experiments were conducted for 10 h with DI water as FS and fertilizer as DS. In order to investigate the OMPs transport behaviors in FDFO, 10 µL of OMPs stock solution was spiked into 1 L FS to obtain a final concentration of 10 µg/L each of four OMPs.

## 2.4 Analytical methods for OMPs

OMPs in samples were analyzed following the procedures described in previous studies [37, 41]. 100 mL samples were prepared and spiked with the corresponding isotopes (Cambridge Isotope Laboratories, Inc., USA) as the internal standards to measure the recovery ratio during the following extraction and evaporation process. OMPs samples were first extracted via solid phase extraction (Dione Autotrace 280 solid-phase extraction instrument and Oasis cartridges) and then concentrated via evaporation. OMPs concentration was then measured by liquid chromatography (Agilent Technology 1260 Infinity Liquid Chromatography unit, USA) connected to mass spectrometry (AB SCIEX QTRAP 5500 mass spectrometer, Applied Biosystems, USA) and each concentration was calculated by comparing its peak area with the peak area of the corresponding isotope (i.e., fixed concentration). OMPs forward flux to DS can be obtained based on mass balance for OMPs species [21, 37].

As the initial OMPs concentration in DS is zero, OMPs mass balance yields:

$$C_{OMPs}(V_{Di} + J_w A_m t) = J_{OMPs} A_m t \quad (1)$$

where  $C_{OMPs}$  is the OMPs concentration in DS ( $\mu\text{g/L}$ ),  $V_{di}$  is the initial DS volume (L),  $J_w$  is the measured water flux ( $\text{L/m}^2/\text{h}$ ),  $A_m$  is the membrane area ( $\text{m}^2$ ),  $t$  is the operation time (h) and  $J_{OMPs}$  is the OMPs forward flux to DS ( $\mu\text{g/m}^2/\text{h}$ ). For OMPs forward flux, **Eq. (1)** can be modified as:

$$J_{OMPs} = \frac{C_{OMPs}(V_{Di} + J_w A_m t)}{A_m t} = \frac{C_{OMPs} V_{Df}}{A_m t} \quad (2)$$

## 2.5 Models for OMPs transport behaviors

### 2.5.1 Pore hindrance transport model

For the pore hindrance transport model, FO membrane should be considered as a bundle of cylindrical capillary tubes having the same radius with the assumption of that the spherical solute particles penetrate FO membrane pores [26]. This model was originally developed to simulate blood flow through individual capillaries [42] and it has been utilized to estimate rejections by size exclusion for porous membranes such as microfiltration and ultrafiltration [39]. Recent studies also applied this model for nano/non-porous membranes such as nanofiltration, reverse osmosis, and forward osmosis [26, 43, 44]. The real rejection of the OMPs was determined using **Eq. (3)** [26, 43].

$$R_r = 1 - \frac{C_p}{C_m} = 1 - \frac{\varphi K_c}{1 - \exp(-P_e(1 - \varphi K_c))} \quad (3)$$

where  $R_r$  is the real rejection of FO membrane,  $C_p$  is the OMPs concentration in the permeate ( $\mu\text{g/L}$ ),  $C_m$  is the OMPs concentration at the membrane surface ( $\mu\text{g/L}$ ),  $\varphi$  is the distribution coefficient,  $K_c$  is the hydrodynamic hindrance coefficient for convection, and  $P_e$  is the membrane Peclet number. The distribution coefficient (**Eq. (4)**) is related to the ratio of OMPs radius to the membrane pore radius (**Eq. (5)**). Peclet number, defined as the ratio of the convective transport rate to the diffusive transport rate, can be obtained from **Eq. (6)**.

$$\varphi = (1 - \lambda)^2 \quad (4)$$

$$\lambda = \frac{r_s}{r_p} \quad (5)$$

$$\text{Pe} = \frac{K_c J_w l}{K_d D \varepsilon} \quad (6)$$

where  $K_d$  is the hydrodynamic hindrance coefficient for diffusion,  $D$  is the Stokes-Einstein diffusion coefficient ( $\text{m}^2/\text{s}$ ),  $l$  is the thickness of the active layer (m), and  $\varepsilon$  is the effective porosity of the active layer. Hydrodynamic hindrance coefficients for convection and diffusion can be determined via **Eq. (7) and (8)** proposed by Bungay and Brenner [42]. It is noteworthy that diffusion can be more dominant to determine solute transports when  $\lambda$  is closed to 1. Details on calculations of hydrodynamic hindrance coefficients are given in elsewhere [42, 43, 45].

$$K_c = \frac{(2-\varphi)K_s}{2K_t} \quad (7)$$

$$K_d = \frac{6\pi}{K_t} \quad (8)$$

### 2.5.2 Relationship between real rejection and observed rejection

Since the real rejection is related to the ratio of the permeate concentration to the membrane surface concentration as **Eq. (3)**, the observed rejection ( $R_o = 1 - c_p/c_f$ ) should be further calculated to obtain OMPs forward flux. The observed rejection can be obtained using the relationship between the real rejection and the observed rejection readily derived from concentration polarization in the film theory [43] as **Eq. (9)**.

$$\ln \frac{(1-R_r)}{R_r} = \ln \frac{(1-R_o)}{R_o} - \frac{J_w}{k} \quad (9)$$

where  $R_o$  is the observed rejection of FO membrane and  $k$  is the mass transfer coefficient for concentration polarization near the active layer (m/s). Details on calculations of mass transfer coefficients are given elsewhere [37].

### 2.5.3 Simulation of OMPs forward flux

To simulate OMPs forward flux, OMPs concentrations in FS and the permeate should be firstly determined. The change in the volume and concentration of FS can be calculated based on mass balance as **Eq. (10)**. For the calculation, water fluxes were employed from experimental data and permeate concentrations were obtained from **Eq. (3)**.

$$\frac{dC_f(t)}{dt} = -\frac{J_w(t)A_m C_p(t)}{V_f(t)} - \frac{C_f(t)}{V_f(t)} \frac{dV_f(t)}{dt} \quad (10)$$

where  $C_f(t)$  is the OMPs concentration in FS ( $\mu\text{g/L}$ ),  $J_w(t)$  is the water flux ( $\text{L/m}^2/\text{h}$ ),  $C_p(t)$  is the OMPs concentration in the permeate ( $\mu\text{g/L}$ ), and  $V_f(t)$  is the volume of FS (L). All parameters varied with respect to operation time. OMPs concentration in DS should be further determined to obtain average OMPs forward flux. Similarly, the change in the volume and concentration of DS can be calculated using **Eq. (11)** derived based on mass balance. Then, average OMPs forward flux can be lastly obtained via **Eq. (12)**.

$$\frac{dC_d(t)}{dt} = \frac{J_w(t)A_m C_p(t)}{V_d(t)} - \frac{C_d(t)}{V_d(t)} \frac{dV_d(t)}{dt} \quad (11)$$

$$J_{s,OMPs}(t) = \frac{C_d(t)V_d(t)}{A_m} \quad (12)$$

where  $C_d(t)$  is the OMPs concentration in DS ( $\mu\text{g/L}$ ),  $V_d(t)$  is the volume of DS (L), and  $J_{s,OMPs}(t)$  is the average OMPs forward flux ( $\mu\text{g/m}^2/\text{L}$ ).

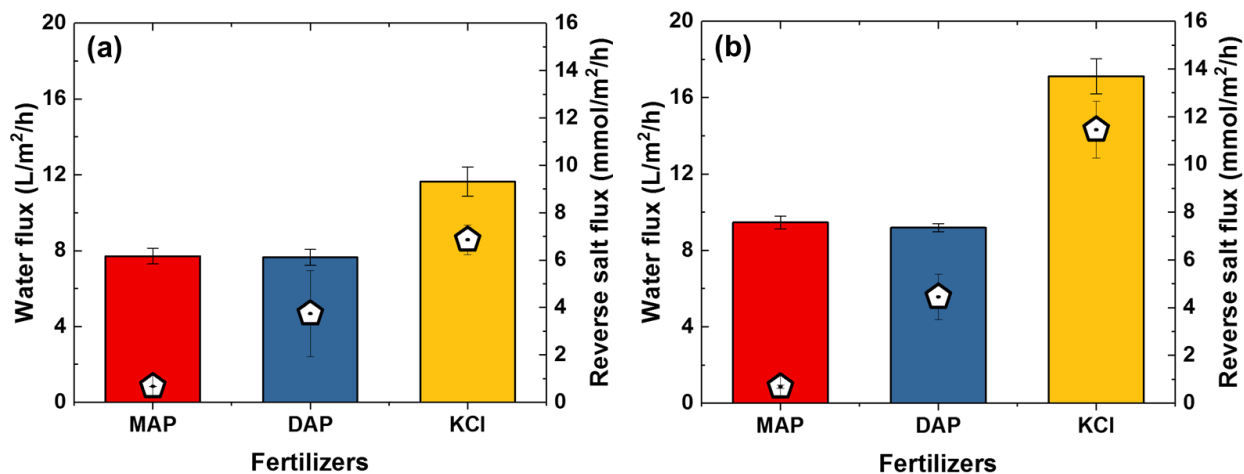
## 3. Results and discussion

### 3.1 FDFO membrane performance

Three different fertilizers (MAP, DAP and KCl) were examined for the performance in FDFO (**Fig. 1**) since MAP and DAP are composed of the same components (N and P) but have different

thermodynamic properties such as osmotic pressure and diffusivity while KCl has a different composition but has a similar osmotic pressure with MAP (**Table S3**). **Fig. 1** shows that MAP exhibited similar water flux with DAP at both 1 M and 2 M DS concentrations, even though DAP has higher osmotic pressure. This is due to lower diffusivity of DAP species which enhances the dilutive ICP effects that lowers the water flux [46]. KCl showed a much higher water flux than MAP despite having similar osmotic pressures, which is attributed to the higher diffusivity of KCl that lowers ICP effects [46]. At a higher DS concentration of 2 M, the water flux for MAP and DAP increased slightly due to increased osmotic pressure (**Table S3**) although the increase was more significant for KCl.

RSF was also investigated for the three DS (**Fig. 1**). KCl showed the highest RSF and this is probably due to its highest solute diffusivity and also lower hydrated diameters of both  $K^+$  and  $Cl^-$  species compared the MAP and DAP [47]. Interestingly, DAP showed much higher RSF than MAP even though they have similar components and DAP has much lower diffusivity as shown in **Table S3**, Supplementary Data. This can probably be explained due to the differences in their species formed in the DS.  $NH_4^+$  ions were much more dominant in DAP, resulting in higher RSF and an increase in FS pH [37]. The RSF for 2 M concentration was correspondingly higher compared to 1 M concentrations.



**Figure 1.** Water flux (columns, left axis) and reverse salt flux (open symbols, right axis) with three fertilizers (i.e., MAP, DAP and KCl) in FDFO at (a) 1 M DS concentration and (b) 2 M DS concentration. Experimental conditions of all FO experiments: DI water as feed solution; crossflow velocity of 8.5 cm/s; and temperature of  $20 \pm 1$  °C.

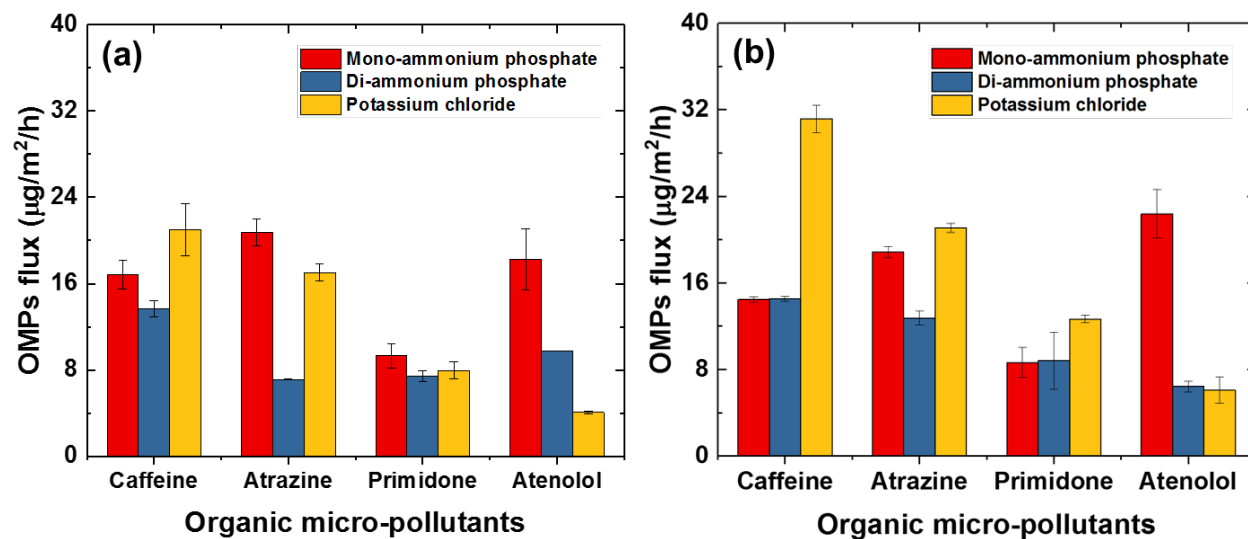
### 3.2 OMPs transport behaviors in fertilizer-drawn forward osmosis

In order to investigate the effect of OMPs surface physicochemical properties on OMPs transport behaviors in the FDFO process, MAP was chosen as DS since it is expected to have less impact on OMPs transport behavior due to lower specific RSF (0.1 mmol/L) compared to other fertilizer DS (i.e., 0.3 mmol/L for DAP and 0.6 mmol/L for KCl) at 1 M DS concentrations. The OMPs transport behaviors were then evaluated by measuring the OMPs forward flux as presented in **Fig. 2**. Primidone showed the lowest OMPs flux (**Fig. 2a**) and therefore the highest rejection rate (**Table S4**, Supplementary Data) followed by caffeine, atenolol and atrazine. It is well known that OMPs transports in membrane-based processes are dominantly influenced by their molecular weights [26, 48, 49], however it is difficult to ascertain a good correlation between the forward OMPs flux and the molecular weight as shown in **Fig. S1a**. Even though atrazine and atenolol



have higher or similar molecular weights than caffeine and primidone, OMPs fluxes of atrazine and atenolol were higher than those of caffeine and primidone. Especially, atrazine exhibited much higher OMPs flux than primidone despite the similar molecular weights (i.e., 216 g/mol and 218 g/mol for atrazine and primidone, respectively).

When the DS concentration was increased from 1 M to 2 M as shown in **Fig. 2b**, the OMPs flux slightly decreased (i.e., reduction ratio: 14.2%, 9.2% and 7.1% for caffeine, atrazine and primidone, respectively) while the trend between the OMPs did not change significantly. However, atenolol exhibited a different behavior as its flux increased from 18.2  $\mu\text{g}/\text{m}^2/\text{h}$  to 22.4  $\mu\text{g}/\text{m}^2/\text{h}$  (increase by 23.1%). Similar to 1 M DS, there was no clear correlation between molecular weight and OMPs flux as presented in **Fig. S1b**. These phenomena is likely due to the different physicochemical properties (i.e., hydrophobicity and surface charges) of OMPs.



**Figure 2.** OMPs flux with three fertilizers (i.e., MAP, DAP and KCl) in FDFO at (a) 1 M DS concentration and (b) 2 M DS concentration. Experimental conditions of all FO experiments: DI water as feed solution; crossflow velocity of 8.5 cm/s; and temperature of  $20 \pm 1$  °C.

To further investigate the effect of DS properties on OMPs transport behaviors, DAP and KCl were employed as DS since DAP exhibited similar water flux with higher RSF and KCl showed both higher water flux and RSF compared to MAP as discussed in **Section 3.1**. When using 1 M DAP DS, atrazine exhibited the lowest OMPs flux (**Fig. 2a**) and the highest rejection rate (**Table S4**) followed by primidone, atenolol and caffeine. Compared with those of 1 M MAP DS, OMPs fluxes were over all reduced (i.e., reduction ratio: 18.8%, 65.7%, 20.1% and 46.4% for caffeine, atrazine, primidone and atenolol, respectively). This might be due to the combined effect of enhanced RSF and increased FS pH on OMPs transport behaviors as presented in **Section 3.1**.

When increasing DS concentration from 1 M to 2 M, the OMPs fluxes increased by 5.7%, 164.6%, 16.3% and 129.2% for caffeine, atrazine, primidone and atenolol, respectively. This might be due to enhanced water flux of 9.2 L/m<sup>2</sup>/h at 2 M DAP from 7.6 L/m<sup>2</sup>/h at 1 M. Increased permeation drag force could deteriorate external concentration polarization, thereby increasing OMPs forward flux. Comparing the DAP with MAP as DS, only atrazine and atenolol exhibited noticeable changes in OMPs forward flux. This result also therefore supports that an increase in RSF and FS pH has more significant effect on transports of hydrophobic and positively charged OMPs.

FO experiments were carried out using 1 M KCl DS to investigate the effect of the degree of RSF on OMPs transport behaviors. Results show that atenolol exhibited the lowest OMPs flux (4.1 µg/m<sup>2</sup>/h) followed by primidone, atrazine and caffeine, which is lower (i.e., reduction ratio: 18%, 14.4% and 77.8% for atrazine, primidone and atenolol, respectively) than those with 1 M MAP DS despite enhanced permeation drag force (50.9%), while OMPs flux of caffeine was higher (i.e., increasing ratio: 24.6%) than that with 1 M MAP DS. This may be because OMPs flux can be dominantly influenced by operation factors such as water flux and RSF and physicochemical

properties of OMPs such as the molecular size. When KCl DS concentration was further increased to 2 M, the results in **Fig. 2b** show that Atenolol had the lowest OMPs flux followed by primidone, atrazine and cafferene, similar to the trend of 1 M KCl DS. It is interesting to therefore note that DS with high RSF showed better linear correlation between OMPs flux and molecular weight as shown in **Fig. S1**, Supplementary Data.

### **3.3 Modelling OMPs transports by pore hindrance model: Transport mechanisms in FDFO**

#### **3.3.1 Effect of OMPs physicochemical properties on OMPs transport behaviors**

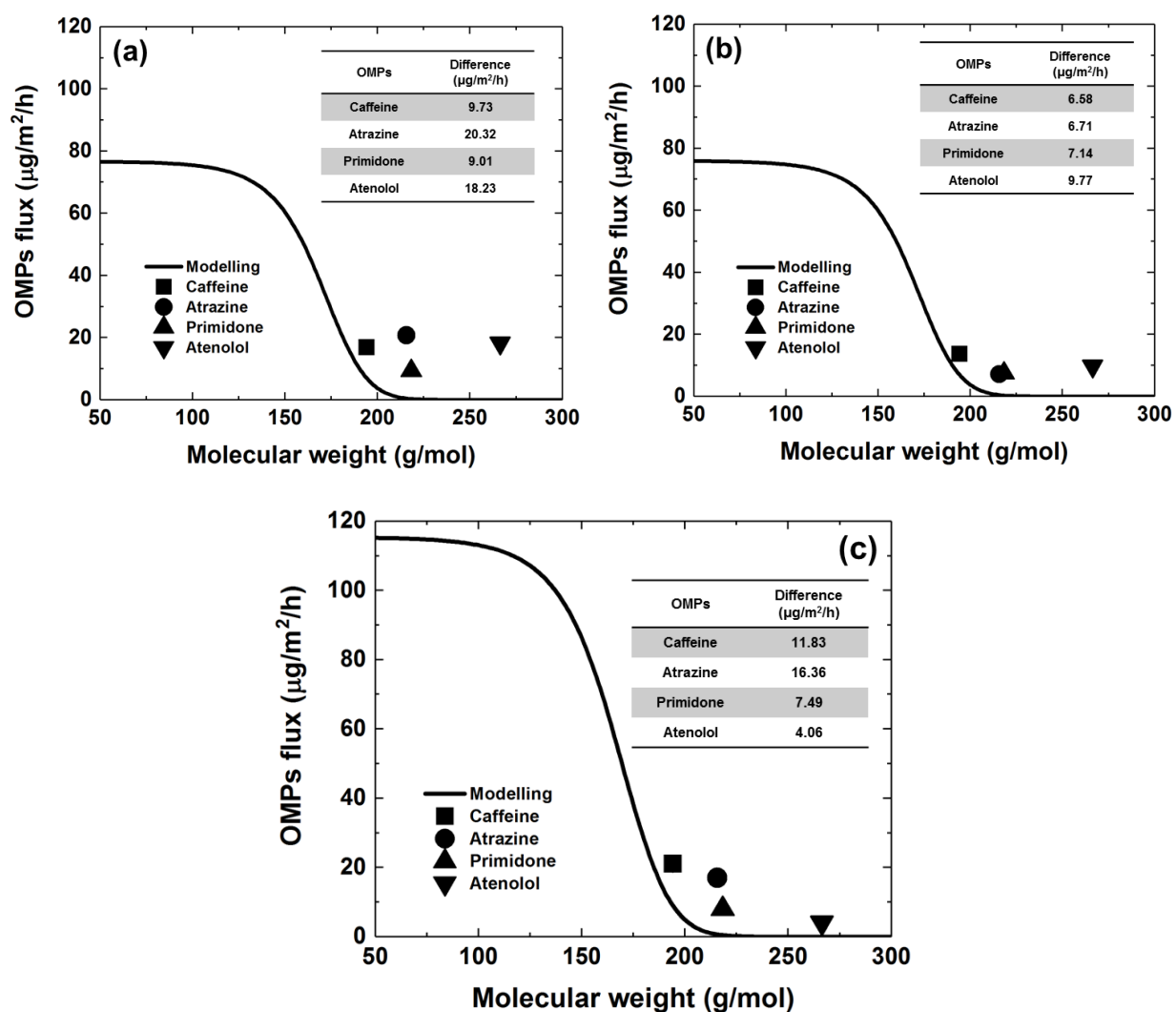
For the more detailed investigation of OMPs transport behaviors in the FDFO process, OMPs forward fluxes were further simulated via the pore hindrance model and mass balance, and compared with the experimental data. To elucidate the effect of physicochemical properties on OMPs transports, OMPs flux with 1 M MAP DS was firstly modelled and presented in **Fig. 3a**. Interestingly, the forward flux of all OMPs was increased because the pore hindrance model considers only steric hindrance between OMPs and FO membrane, and their chemical properties were not considered. Results in **Fig. 3a** (Table inside) show that atrazine and atenolol exhibited higher difference between modelled and experimental OMPs flux than caffeine and primidone. This difference might be originated from the different physicochemical properties (i.e., hydrophobicity and surface charges) of OMPs as depicted in **Fig. 4a**. The surfaces of caffeine, atrazine and primidone have not only similar neutral charges but also different hydrophobicity (**Table 1**). Particularly, atrazine has the high hydrophobic surface, thereby possibly inducing the adsoption of atrazine on the membrane surface, and thus, enhancing the OMPs transport through moderately hydrophilic FO membrane (contact angle of the active layer of FO membrane of 79.5°

(**Table 2**). To further confirm this hypothesis, the adsorbed amounts of OMPs were calculated based on mass balance and presented in **Table 3**. Atrazine among three OMPs with the neutrally charged surface exhibited the highest adsorbed amount (i.e., 2.79 mg/m<sup>2</sup>, 0.17 mg/m<sup>2</sup> and 1.27 mg/m<sup>2</sup> for atrazine, caffeine and primidone, respectively), which results in higher concentration at the active layer. Therefore, it held true that the hydrophobic interaction could be the dominant mechanism for the transport behavior of Atrazine. Besides, when the surface hydrophobicity was similar (i.e., caffeine and primidone), caffeine showed higher OMPs flux than primidone, implying that molecular weight could be the dominant factor to determine the forward flux of OMPs.

**Table 3.** Adsorbed amounts of OMPs on the membrane surface. Adsorbed amounts of OMPs were estimated via simple mass balance.

	Caffeine	Atrazine	Primidone	Atenolol
Adsorbed amount (mg/m <sup>2</sup> )	0.17	2.79	1.27	3.31

In addition to hydrophobicity, surface charges of OMPs can significantly affect the OMPs transport behavior via electrostatic repulsion or electrostatic attraction with membranes that contain surface charges [25]. **Fig. 2a** shows that atenolol exhibits high forward OMPs flux despite its high molecular weight. This might be due to the electrostatic attraction caused by the positively charged surface of atenolol and the negatively charged surface of FO membrane as shown in **Table 1** and **Table 2**. In **Table 3**, atenolol has the highest amount of OMPs (3.31 mg/m<sup>2</sup>) adsorbed on the membrane surface. Thus, it could induce high OMPs concentration gradient across the active layer, thereby enhancing the forward flux of atrazine.



**Figure 3.** Model prediction (solid line) for OMPs flux as a function of solute molecular weight based on the pore hindrance transport model for (a) MAP DS, (b) DAP DS, and (c) KCl DS at 1 M DS concentration. Also included are measured solute forward fluxes of four OMPs (i.e., caffeine, atrazine, primidone and atenolol). Tables in each panel indicate the difference between modelled OMPs flux and experimental data. The relevant parameters in **Table 1** and **Table S2** were used in the model calculations. Other parameters used in modelling were employed from experimental data presented in **Fig. 1a**.

### 3.3.2 Effect of alkaline fertilizer DS (DAP) on OMPs transport behaviors

To investigate the effect of alkaline fertilizer DS (DAP) on the transport behavior of OMPs in FDFO, OMPs flux with 1 M DAP DS was simulated using experimental average water flux, presented in **Fig. 3b**. The differences between modelled OMPs flux and experimental data of all OMPs were decreased but the forward fluxes of atrazine and atenolol were further reduced compared to 1 M MAP DS. This could be due to an enhancement of RSF with similar water flux [20]. DAP DS has higher RSF (i.e., 2.5 mmol/m<sup>2</sup>/h and 0.7 mmol/m<sup>2</sup>/h, respectively) than MAP DS while water flux is very similar (i.e., 7.6 L/m<sup>2</sup>/h and 7.7 L/m<sup>2</sup>/h, respectively) as shown in **Fig. 1a**. Higher reverse diffusion of draw solutes could hinder the transport of feed solutes through the FO membrane, resulting in lower OMPs forward flux. In addition, DAP DS increase FS pH by up to 9.17 during 10 h of operation and this could potentially change the membrane surface properties (i.e., decreasing contact angle and slightly increasing zeta potential) of FO membrane due to hydrophilic surface functional groups [25]. Particularly, a reduction in contact angle suggested the hydration swelling of the active layer [50]. Hence, atrazine cannot readily approach to FO membrane due to steric hindrance by water molecules on the membrane surface, making hydrophobic interaction negligible (**Fig. 4b**). As a result, OMPs (i.e., atrazine and primidone) with similar molecular weight but different surface properties exhibited similar OMPs flux.

For atenolol, an increase in FS pH to 9.17 could change the surface charge from positive charges to neutral charges owing to pKa 9.6. Therefore Atenolol could be less adsorbed on the active layer and thus less transported into DS (**Fig. 4b**). To verify this hypothesis, adsorbed amounts of atenolol were calculated vis mass balance. They were 3.31 mg/m<sup>2</sup> and 2.27 mg/m<sup>2</sup> for MAP 1 M and DAP 1 M, respectively, which is similar to other study that atenolol adsorption (the retardation factor) on a sandy aquifer material decreased from 23.3 to 15.8 as pH increased from 4 to 8 [51]. To

confirm the effect of DAP DS on the transport of OMPs in FDFO, OMPs flux with 2 M DAP DS was also simulated using experimental average water flux and presented in **Fig. S2b**. The trend of **Fig. S2b** was consistent with that of **Fig. 3b**, indicating that OMPs transport behavior is dominantly influenced by enhanced steric hindrance due to increased RSF and a change in the surface properties of both FO membrane and OMPs by increased pH in FS.

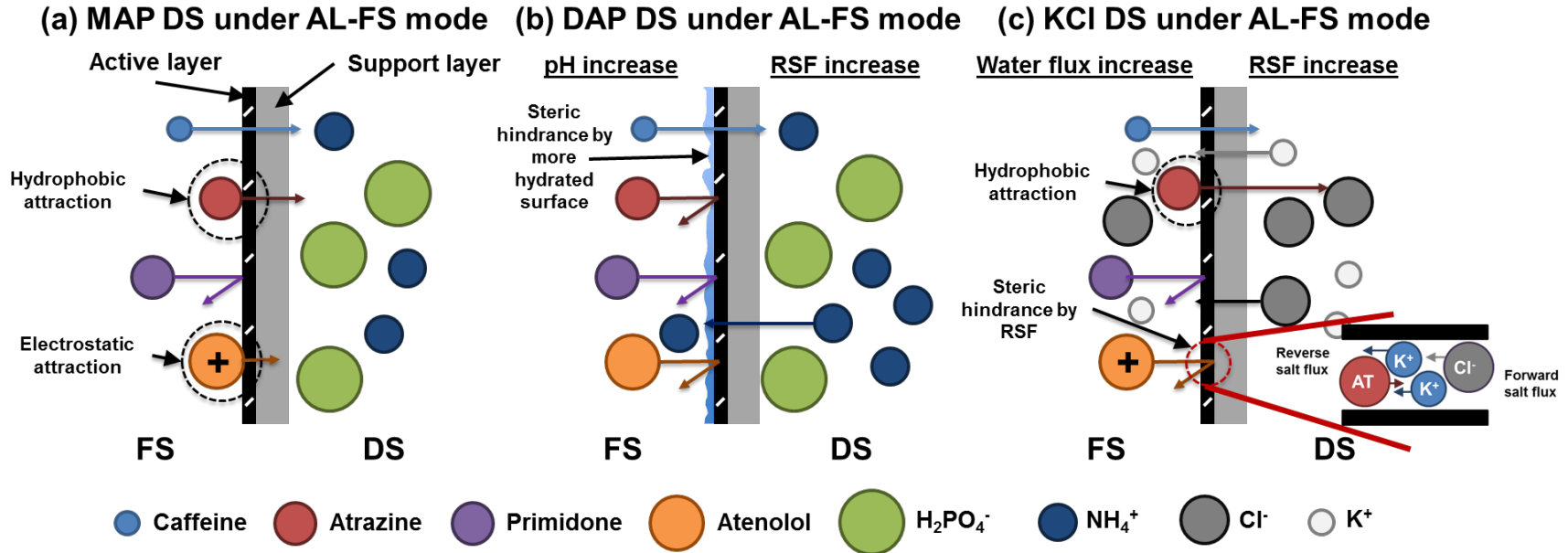
### 3.3.3 Effect of DS having high RSF (KCl) on OMPs transport behaviors

Lastly, the simulation of OMPs flux with 1 M KCl DS was carried out using experimental data to understand the transport behavior with KCl DS (i.e., high water flux and high RSF). Results indicate that modelled OMPs flux with KCl DS is noticeably increased compared to MAP DS and DAP DS. This is due to higher water flux of KCl DS than those of other fertilizer DS. When comparing modelled OMPs flux with experimental OMPs flux, atenolol exhibited the lowest difference followed by primidone, caffeine and atrazine (**Fig. 3c**), indicating that OMPs with high molecular weights are more readily influenced by high RSF. Therefore, it can be hypothesized that the forward flux of OMPs are dominantly determined by the interplay among water flux, RSF and the molecular size of OMPs. High water flux could cause an enhanced external concentration polarization, thereby potentially leading to an increased flux of OMPs [52]. Hence, caffeine with low molecular weight could be more readily transported to the DS. In addition, the transport of OMPs is significantly influenced by their molecular weights due to the hindrance effect of RSF as shown in **Fig. 4c**. Consequently, the forward flux of OMPs with high molecular weight in 1 M KCl DS became lower than that in 1 M MAP DS. **Fig. S1c** indicates that the forward OMPs flux becomes a function of molecular weights when using 1 M KCl DS.

To validate this hypothesis, OMPs forward fluxes with 2 M KCl DS (**Fig. S1c**) were further compared with those with 2 M MAP DS (**Fig. S1a**). Results show that the forward fluxes of three OMPs except for atenolol were increased, supporting the transport mechanism that the transport of OMPs having high molecular weight are more readily affected by RSF when high water flux. It is noteworthy that the removal rates of all OMPs were increased when comparing KCl DS with MAP DS (**Table S4**). This phenomenon agrees well with the results from other studies that high water flux leads to a decrease in removal rates due to the dilution effect [22, 53]. Interestingly, the trend of three OMPs (i.e., Caffeine, Atrazine and Primidone) with neutral surface was similar to that with MAP DS rather than DAP DS. The reverse diffusion of KCl DS could not influence FS pH and thus the surface chemical property of FO membrane was a dominant factor to determine the transport of OMPs having relatively low molecular weight.

Findings from the present study have significant implications for optimizing FDFO process for treatment of wastewater containing OMPs. When using MAP and KCl as DS, rejections of OMPs were significantly governed by the surface physicochemical property of OMPs. However, DAP DS could reject most OMPs effectively due to increased FS pH by the back diffusion of  $\text{NH}_4^+$  in DS. This implies that alkaline DS is recommended for the effective removal of OMPs in wastewater, consistent with other study [54] evaluated boron using high pH DS. In this study, experimental OMPs fluxes were higher than theoretical OMPs fluxes obtained based on the pore hindrance model since the solution-diffusion model is dominant for non-porous membranes such as NF, RO and FO membranes. Nevertheless, the pore hindrance model can help in understanding how the surface properties of OMPs and FO membrane influence the OMPs transport behaviors because it considers only the steric hindrance effect by size exclusion.





**Figure 4.** Schematic description of OMPs transport mechanisms in FO. RSF plays an important role to determine OMPs transports. With MAP DS having low RSF, OMPs transports are dominantly influenced by their properties (i.e., molecular weights, surface charges, and surface hydrophobicity). With DAP DS having intermediate RSF, an increase in FS pH can alter the surface physicochemical property of both FO membrane and OMPs and hence significantly influence OMPs transport. With KCl DS having high RSF, the transport behavior of OMPs are more readily affected by both high RSF and the surface properties of OMPs.

## 4. Conclusions

We systematically investigated the OMPs transport mechanisms in the FDFO using four different OMPs having different molecular weights and surface physicochemical characteristics with three different fertilizers as DS. The OMPs' transport behaviors were simulated using the pore hindrance transport model to identify the effect of OMPs surface physicochemical properties on OMPs transports. The primary findings drawn from this study can be summarized briefly as follows:

- KCl showed the highest water flux and RSF while MAP and DAP exhibited similar water flux but different RSF.
- When using MAP and KCl DS (moderate water flux and low RSF), the physicochemical properties (i.e., hydrophobicity and surface charge) of OMPs determined the transport behavior of OMPs. The remarkably increased RSF using KCl could hamper the transport of OMPs having high molecular weight.
- With DAP DS, FO membrane was more hydrated by increased pH as well as enhanced RSF could more readily hinder the transports of OMPs through FO membrane and thus rejections of all OMPs were enhanced.
- The pore hindrance model was instrumental for understanding the effects of the hydrodynamic properties and the physicochemical properties on OMPs transports

## Acknowledgements

This research was supported by funding from the SEED program of King Abdullah University of Science and Technology (KAUST), Saudi Arabia. The help, assistance and support of the Water Desalination and Reuse Center (WDRC) staff are greatly appreciated.

## References

- [1] S.A. Snyder, P. Westerhoff, Y. Yoon, D.L. Sedlak, Pharmaceuticals, Personal Care Products, and Endocrine Disruptors in Water: Implications for the Water Industry, *Environmental Engineering Science*, 20 (2003) 449-469.
- [2] M. Arslan, I. Ullah, J.A. Müller, N. Shahid, M. Afzal, Organic Micropollutants in the Environment: Ecotoxicity Potential and Methods for Remediation, in: N.A. Anjum, S.S. Gill, N. Tuteja (Eds.) *Enhancing Cleanup of Environmental Pollutants: Volume 1: Biological Approaches*, Springer International Publishing, Cham, 2017, pp. 65-99.
- [3] J.Y.M. Tang, S. McCarty, E. Glenn, P.A. Neale, M.S.J. Warne, B.I. Escher, Mixture effects of organic micropollutants present in water: Towards the development of effect-based water quality trigger values for baseline toxicity, *Water Research*, 47 (2013) 3300-3314.
- [4] M.O. Barbosa, N.F.F. Moreira, A.R. Ribeiro, M.F.R. Pereira, A.M.T. Silva, Occurrence and removal of organic micropollutants: An overview of the watch list of EU Decision 2015/495, *Water Research*, 94 (2016) 257-279.
- [5] B.I. Escher, M. Allinson, R. Altenburger, P.A. Bain, P. Balaguer, W. Busch, J. Crago, N.D. Denslow, E. Dopp, K. Hilscherova, A.R. Humpage, A. Kumar, M. Grimaldi, B.S. Jayasinghe, B. Jarosova, A. Jia, S. Makarov, K.A. Maruya, A. Medvedev, A.C. Mehinto, J.E. Mendez, A. Poulsen, E. Prochazka, J. Richard, A. Schifferli, D. Schlenk, S. Scholz, F. Shiraishi, S. Snyder, G. Su, J.Y.M. Tang, B.v.d. Burg, S.C.v.d. Linden, I. Werner, S.D. Westerheide, C.K.C. Wong, M. Yang, B.H.Y. Yeung, X. Zhang, F.D.L. Leusch, Benchmarking Organic Micropollutants in Wastewater, Recycled Water and Drinking Water with In Vitro Bioassays, *Environmental Science & Technology*, 48 (2014) 1940-1956.
- [6] H. Jeong, C. Seong, T. Jang, S. Park, Classification of Wastewater Reuse for Agriculture: A Case Study in South Korea, *Irrigation and Drainage*, 65 (2016) 76-85.
- [7] M. Bernhard, J. Müller, T.P. Knepper, Biodegradation of persistent polar pollutants in wastewater: Comparison of an optimised lab-scale membrane bioreactor and activated sludge treatment, *Water Research*, 40 (2006) 3419-3428.
- [8] C. Grandclément, I. Seyssiecq, A. Piram, P. Wong-Wah-Chung, G. Vanot, N. Tiliacos, N. Roche, P. Doumenq, From the conventional biological wastewater treatment to hybrid processes, the evaluation of organic micropollutant removal: A review, *Water Research*, 111 (2017) 297-317.
- [9] S. Pérez, P. Eichhorn, D.S. Aga, Evaluating the biodegradability of sulfamethazine, sulfamethoxazole, sulfathiazole, and trimethoprim at different stages of sewage treatment, *Environmental Toxicology and Chemistry*, 24 (2005) 1361-1367.

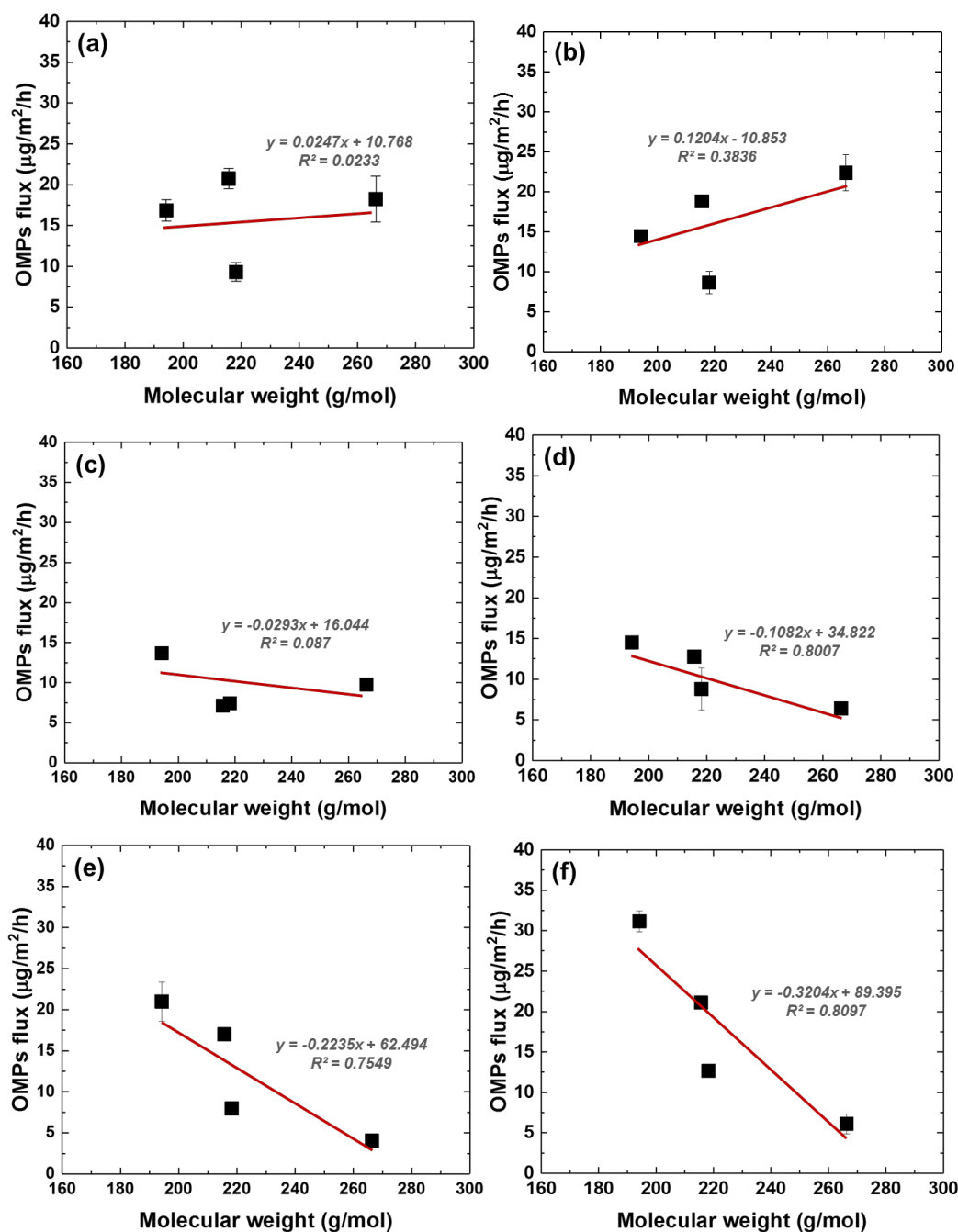
- [10] M. Carballa, F. Omil, J.M. Lema, M.a. Llompарт, C. García-Jares, I. Rodríguez, M. Gómez, T. Ternes, Behavior of pharmaceuticals, cosmetics and hormones in a sewage treatment plant, *Water Research*, 38 (2004) 2918-2926.
- [11] M. Clara, B. Strenn, O. Gans, E. Martinez, N. Kreuzinger, H. Kroiss, Removal of selected pharmaceuticals, fragrances and endocrine disrupting compounds in a membrane bioreactor and conventional wastewater treatment plants, *Water Research*, 39 (2005) 4797-4807.
- [12] F.I. Hai, K. Tessmer, L.N. Nguyen, J. Kang, W.E. Price, L.D. Nghiem, Removal of micropollutants by membrane bioreactor under temperature variation, *Journal of Membrane Science*, 383 (2011) 144-151.
- [13] D.o.E.a.C. (NSW), Environmental Guidelines: Use of Effluent by Irrigation, Department of Environment and Conservation (NSW), 2004.
- [14] M.A. Shannon, P.W. Bohn, M. Elimelech, J.G. Georgiadis, B.J. Mariñas, A.M. Mayes, Science and technology for water purification in the coming decades, *Nature*, 452 (2008) 301.
- [15] T. Fujioka, S.J. Khan, J.A. McDonald, L.D. Nghiem, Rejection of trace organic chemicals by a nanofiltration membrane: the role of molecular properties and effects of caustic cleaning, *Environmental Science: Water Research & Technology*, 1 (2015) 846-854.
- [16] J. Radjenović, M. Petrović, F. Ventura, D. Barceló, Rejection of pharmaceuticals in nanofiltration and reverse osmosis membrane drinking water treatment, *Water Research*, 42 (2008) 3601-3610.
- [17] P. Xu, J.E. Drewes, C. Bellona, G. Amy, T.U. Kim, M. Adam, T. Heberer, Rejection of emerging organic micropollutants in nanofiltration-reverse osmosis membrane applications, *Water environment research : a research publication of the Water Environment Federation*, 77 (2005) 40-48.
- [18] T.H. Chong, S.-L. Loo, W.B. Krantz, Energy-efficient reverse osmosis desalination process, *Journal of Membrane Science*, 473 (2015) 177-188.
- [19] S. Lee, C. Boo, M. Elimelech, S. Hong, Comparison of fouling behavior in forward osmosis (FO) and reverse osmosis (RO), *Journal of Membrane Science*, 365 (2010) 34-39.
- [20] M. Xie, L.D. Nghiem, W.E. Price, M. Elimelech, Comparison of the removal of hydrophobic trace organic contaminants by forward osmosis and reverse osmosis, *Water Research*, 46 (2012) 2683-2692.
- [21] C. Kim, S. Lee, H.K. Shon, M. Elimelech, S. Hong, Boron transport in forward osmosis: Measurements, mechanisms, and comparison with reverse osmosis, *Journal of Membrane Science*, 419-420 (2012) 42-48.

- [22] M. Xie, W.E. Price, L.D. Nghiem, M. Elimelech, Effects of feed and draw solution temperature and transmembrane temperature difference on the rejection of trace organic contaminants by forward osmosis, *Journal of Membrane Science*, 438 (2013) 57-64.
- [23] X. Jin, Q. She, X. Ang, C.Y. Tang, Removal of boron and arsenic by forward osmosis membrane: Influence of membrane orientation and organic fouling, *Journal of Membrane Science*, 389 (2012) 182-187.
- [24] A.A. Alturki, J.A. McDonald, S.J. Khan, W.E. Price, L.D. Nghiem, M. Elimelech, Removal of trace organic contaminants by the forward osmosis process, *Separation and Purification Technology*, 103 (2013) 258-266.
- [25] M. Xie, W.E. Price, L.D. Nghiem, Rejection of pharmaceutically active compounds by forward osmosis: Role of solution pH and membrane orientation, *Separation and Purification Technology*, 93 (2012) 107-114.
- [26] M. Xie, L.D. Nghiem, W.E. Price, M. Elimelech, Relating rejection of trace organic contaminants to membrane properties in forward osmosis: Measurements, modelling and implications, *Water Research*, 49 (2014) 265-274.
- [27] M. Xie, L.D. Nghiem, W.E. Price, M. Elimelech, Impact of organic and colloidal fouling on trace organic contaminant rejection by forward osmosis: Role of initial permeate flux, *Desalination*, 336 (2014) 146-152.
- [28] R. Valladares Linares, V. Yangali-Quintanilla, Z. Li, G. Amy, Rejection of micropollutants by clean and fouled forward osmosis membrane, *Water Research*, 45 (2011) 6737-6744.
- [29] L. Chekli, S. Phuntsho, J.E. Kim, J. Kim, J.Y. Choi, J.-S. Choi, S. Kim, J.H. Kim, S. Hong, J. Sohn, H.K. Shon, A comprehensive review of hybrid forward osmosis systems: Performance, applications and future prospects, *Journal of Membrane Science*, 497 (2016) 430-449.
- [30] J.E. Kim, S. Phuntsho, S.M. Ali, J.Y. Choi, H.K. Shon, Forward osmosis membrane modular configurations for osmotic dilution of seawater by forward osmosis and reverse osmosis hybrid system, *Water Research*, 128 (2018) 183-192.
- [31] Y. Kim, Y.C. Woo, S. Phuntsho, L.D. Nghiem, H.K. Shon, S. Hong, Evaluation of fertilizer-drawn forward osmosis for coal seam gas reverse osmosis brine treatment and sustainable agricultural reuse, *Journal of Membrane Science*, 537 (2017) 22-31.
- [32] Y. Kim, L. Chekli, W.-G. Shim, S. Phuntsho, S. Li, N. Ghaffour, T. Leiknes, H.K. Shon, Selection of suitable fertilizer draw solute for a novel fertilizer-drawn forward osmosis-anaerobic membrane bioreactor hybrid system, *Bioresource Technology*, 210 (2016) 26-34.

- [33] L. Chekli, Y. Kim, S. Phuntsho, S. Li, N. Ghaffour, T. Leiknes, H.K. Shon, Evaluation of fertilizer-drawn forward osmosis for sustainable agriculture and water reuse in arid regions, *Journal of Environmental Management*, 187 (2017) 137-145.
- [34] S. Li, Y. Kim, S. Phuntsho, L. Chekli, H.K. Shon, T. Leiknes, N. Ghaffour, Methane production in an anaerobic osmotic membrane bioreactor using forward osmosis: Effect of reverse salt flux, *Bioresource Technology*, 239 (2017) 285-293.
- [35] Y. Kim, S. Li, L. Chekli, S. Phuntsho, N. Ghaffour, T. Leiknes, H.K. Shon, Influence of fertilizer draw solution properties on the process performance and microbial community structure in a side-stream anaerobic fertilizer-drawn forward osmosis – ultrafiltration bioreactor, *Bioresource Technology*, 240 (2017) 149-156.
- [36] S. Li, Y. Kim, L. Chekli, S. Phuntsho, H.K. Shon, T. Leiknes, N. Ghaffour, Impact of reverse nutrient diffusion on membrane biofouling in fertilizer-drawn forward osmosis, *Journal of Membrane Science*, 539 (2017) 108-115.
- [37] Y. Kim, S. Li, L. Chekli, Y.C. Woo, C.-H. Wei, S. Phuntsho, N. Ghaffour, T. Leiknes, H.K. Shon, Assessing the removal of organic micro-pollutants from anaerobic membrane bioreactor effluent by fertilizer-drawn forward osmosis, *Journal of Membrane Science*, 533 (2017) 84-95.
- [38] L. Chekli, J.E. Kim, I. El Saliby, Y. Kim, S. Phuntsho, S. Li, N. Ghaffour, T. Leiknes, H. Kyong Shon, Fertilizer drawn forward osmosis process for sustainable water reuse to grow hydroponic lettuce using commercial nutrient solution, *Separation and Purification Technology*, 181 (2017) 18-28.
- [39] V.G.J. Rodgers, K.D. Miller, Analysis of steric hindrance reduction in pulsed protein ultrafiltration, *Journal of Membrane Science*, 85 (1993) 39-58.
- [40] C.R. Wilke, P. Chang, Correlation of diffusion coefficients in dilute solutions, *AIChE Journal*, 1 (1955) 264-270.
- [41] C.-H. Wei, C. Hoppe-Jones, G. Amy, T. Leiknes, Organic micro-pollutants' removal via anaerobic membrane bioreactor with ultrafiltration and nanofiltration, *Journal of Water Reuse and Desalination*, (2015).
- [42] P.M. Bungay, H. Brenner, The motion of a closely-fitting sphere in a fluid-filled tube, *International Journal of Multiphase Flow*, 1 (1973) 25-56.
- [43] L.D. Nghiem, A.I. Schäfer, M. Elimelech, Removal of Natural Hormones by Nanofiltration Membranes: Measurement, Modeling, and Mechanisms, *Environmental Science & Technology*, 38 (2004) 1888-1896.
- [44] Y. Yoon, R.M. Lueptow, Removal of organic contaminants by RO and NF membranes, *Journal of Membrane Science*, 261 (2005) 76-86.

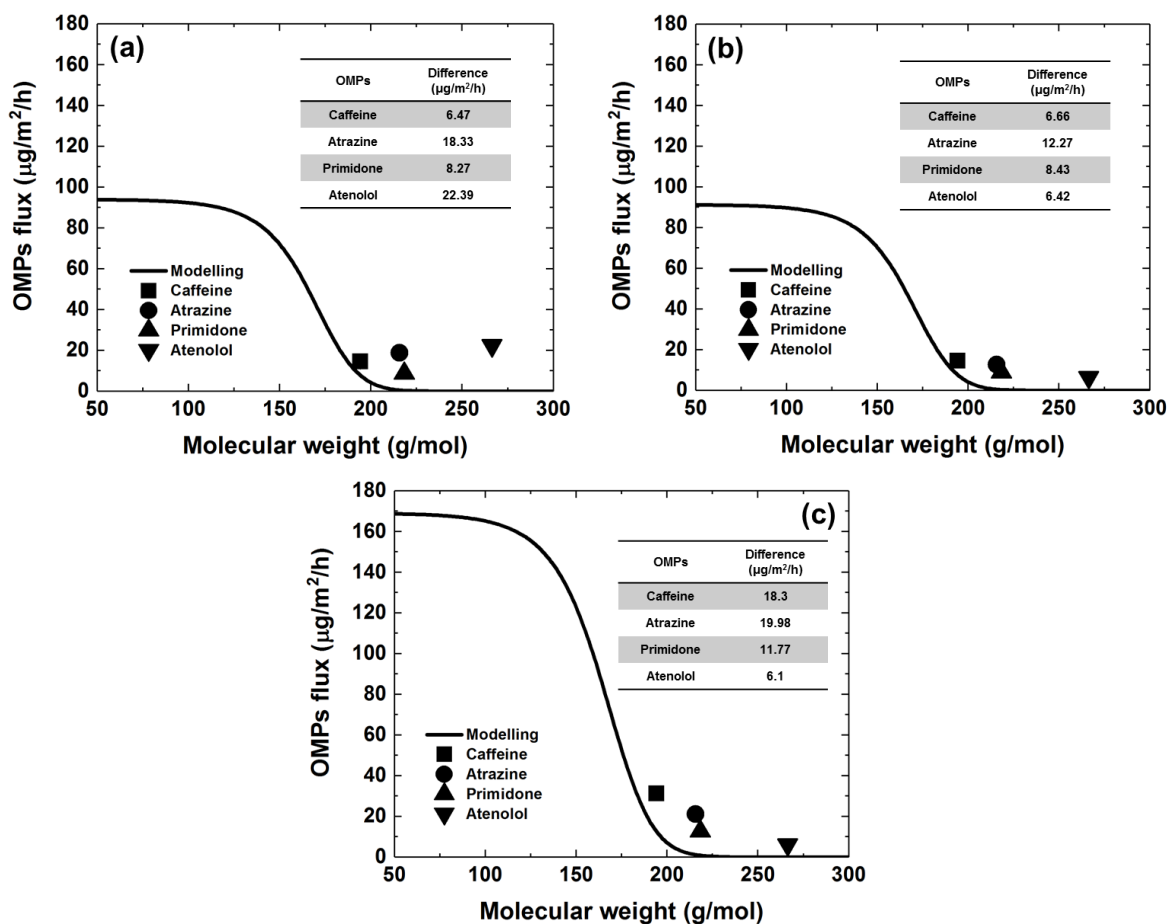
- [45] J. Wang, D.S. Dlamini, A.K. Mishra, M.T.M. Pendergast, M.C.Y. Wong, B.B. Mamba, V. Freger, A.R.D. Verliefde, E.M.V. Hoek, A critical review of transport through osmotic membranes, *Journal of Membrane Science*, 454 (2014) 516-537.
- [46] Y. Kim, S. Lee, H.K. Shon, S. Hong, Organic fouling mechanisms in forward osmosis membrane process under elevated feed and draw solution temperatures, *Desalination*, 355 (2015) 169-177.
- [47] A. Achilli, T.Y. Cath, A.E. Childress, Selection of inorganic-based draw solutions for forward osmosis applications, *Journal of Membrane Science*, 364 (2010) 233-241.
- [48] Y. Kiso, Y. Sugiura, T. Kitao, K. Nishimura, Effects of hydrophobicity and molecular size on rejection of aromatic pesticides with nanofiltration membranes, *Journal of Membrane Science*, 192 (2001) 1-10.
- [49] K. Kimura, S. Toshima, G. Amy, Y. Watanabe, Rejection of neutral endocrine disrupting compounds (EDCs) and pharmaceutical active compounds (PhACs) by RO membranes, *Journal of Membrane Science*, 245 (2004) 71-78.
- [50] A.L. Ahmad, L.S. Tan, S.R. Abd. Shukor, The role of pH in nanofiltration of atrazine and dimethoate from aqueous solution, *Journal of Hazardous Materials*, 154 (2008) 633-638.
- [51] M. Schaffer, N. Boxberger, H. Börnick, T. Licha, E. Worch, Sorption influenced transport of ionizable pharmaceuticals onto a natural sandy aquifer sediment at different pH, *Chemosphere*, 87 (2012) 513-520.
- [52] Y. Kim, S. Li, L. Chekli, Y.C. Woo, C.-H. Wei, S. Phuntsho, N. Ghaffour, T. Leiknes, H.K. Shon, Assessing the removal of organic micro-pollutants from anaerobic membrane bioreactor effluent by fertilizer-drawn forward osmosis, *Journal of Membrane Science*, 533 (2017) 84-95.
- [53] S. Lee, G. Amy, J. Cho, Applicability of Sherwood correlations for natural organic matter (NOM) transport in nanofiltration (NF) membranes, *Journal of Membrane Science*, 240 (2004) 49-65.
- [54] Y.-N. Wang, W. Li, R. Wang, C.Y. Tang, Enhancing boron rejection in FO using alkaline draw solutions, *Water Research*, 118 (2017) 20-25.

## Supplementary Information



**Figure S1.** Relationship of molecular weights of OMPs with OMPs flux: (a) 1 M MAP DS, (b) 2 M MAP DS, (c) 1 M DAP DS, (d) 2 M DAP DS, (e) 1 M KCl DS, and (f) 2 M KCl DS.





**Figure S2.** Model prediction (solid line) for OMPs flux as a function of solute molecular weight based on the pore hindrance transport model for (a) MAP DS, (b) DAP DS, and (c) KCl DS at 2 M DS concentration. Also included are measured solute forward fluxes of four OMPs (i.e., Caffeine, Atrazine, Primidone and Atenolol). Tables in figures indicate the difference between modelled OMPs flux and experimental data. The relevant parameters in **Table 1** and **Table S2** were used in the model calculations. Other parameters used in modelling were employed from experimental data presented in **Fig. 3a**.

**Table S1.** Experimental data for HTI CTA FO membrane properties (i.e., water and salt (NaCl) permeability coefficients of the active layer and the structural parameter of the support layer) adopted from our previous study [32].

	Water permeability coefficient, A	Salt permeability coefficient, B	Structural parameter, S
HTI CTA FO membrane	0.368 L/m <sup>2</sup> /h/bar	0.191 kg/m <sup>2</sup> /h	289.84 $\mu$ m

**Table S2.** Membrane radius ( $r_p$ ) and structural factor ( $l/\varepsilon$ ) of HTI CTA FO membrane adopted from other study [26]. Both values were calculated from the pore hindrance transport model developed for nanofiltration [43].

	Pore radius (nm)	Structural factor ( $l/\varepsilon$ )
HTI CTA FO membrane	$0.37 \pm 0.04$	$0.12 \pm 0.08$

**Table S3.** Details of the fertilizer chemicals used in this study. Thermodynamic properties were determined at temperature of 20 °C by using OLI Stream Analyzer 3.2.

Chemicals	Mono-ammonium phosphate (MAP)		Di-ammonium phosphate (DAP)		Potassium chloride	
Formula	NH <sub>4</sub> H <sub>2</sub> PO <sub>4</sub>		(NH <sub>4</sub> ) <sub>2</sub> HPO <sub>4</sub>		KCl	
Molecular weight (g/mol)	115.0		132.1		74.6	
Concentration	1 M	2 M	1 M	2 M	1 M	2 M
Osmotic pressure (atm)	43.4	86.14	49.85	93.57	43.3	87.95
Diffusivity ( $\times 10^{-9}$ m <sup>2</sup> /s)	1.05	1.08	0.87	0.87	1.59	1.55
Viscosity (mPa • s)	1.33	1.73	1.11	1.20	0.99	0.99

**Table S4.** Permeate OMPs concentration and OMPs rejection with different membrane orientation and draw solution concentration. Observed OMPs rejection was calculated via the following equation,  $R_o = 1 - (c_p \times V_D/V_p)/c_f$ . Experimental conditions for OMPs transport behaviors: DI water with 10 µg/L OMPs as feed solution; crossflow velocity of 8.5 cm/s; 10 h operation; and temperature of  $20 \pm 1$  °C.

		1 M DS concentration			2 M DS concentration		
		MAP	DAP	KCl	MAP	DAP	KCl
<b>Permeate concentration</b>	Caffeine	0.29	0.24	0.34	0.24	0.25	0.46
	Atrazine	0.36	0.12	0.28	0.32	0.22	0.31
	Primidone	0.16	0.13	0.13	0.15	0.15	0.19
	Atenolol	0.32	0.17	0.07	0.38	0.11	0.09
<b>Observed rejection (%)</b>	Caffeine	81.3	84.4	85.5	87.2	86.7	87.2
	Atrazine	76.9	92.0	88.4	83.2	88.3	91.5
	Primidone	89.9	91.6	94.7	92.4	92.0	95.0
	Atenolol	79.8	88.9	97.3	79.8	94.2	97.6

## References

- [1] Y. Kim, L. Chekli, W.-G. Shim, S. Phuntsho, S. Li, N. Ghaffour, T. Leiknes, H.K. Shon, Selection of suitable fertilizer draw solute for a novel fertilizer-drawn forward osmosis–anaerobic membrane bioreactor hybrid system, *Bioresource Technology*, 210 (2016) 26-34.
- [2] M. Xie, L.D. Nghiem, W.E. Price, M. Elimelech, Relating rejection of trace organic contaminants to membrane properties in forward osmosis: Measurements, modelling and implications, *Water Research*, 49 (2014) 265-274.
- [3] L.D. Nghiem, A.I. Schäfer, M. Elimelech, Removal of Natural Hormones by Nanofiltration Membranes: Measurement, Modeling, and Mechanisms, *Environmental Science & Technology*, 38 (2004) 1888-1896.